

# Virtual photon structure at HERA

P. J. Bussey<sup>a</sup>

<sup>a</sup>Department of Physics and Astronomy, University of Glasgow, Glasgow G12 8QQ, United Kingdom  
for the H1 and ZEUS Collaborations

An overview is given of the ongoing measurement at HERA of the parton structure of the photon, as a function of its virtuality. Preliminary ZEUS results show disagreement with an NLO QCD calculation.

## 1. INTRODUCTION

In  $ep$  collisions at HERA, the incoming electron or positron radiates a virtual vector boson which then interacts with the proton. In the hardest high-energy collisions, this boson may be a  $W$  or  $Z$ , but the vast majority of collisions are mediated by a virtual photon. Its virtuality  $Q^2$  varies from a lower limit of  $O(10^{-13} \text{ GeV}^2)$ , given by the mass squared of the electron, to an upper limit of  $O(10^4 \text{ GeV}^2)$  given by the energy of the collider. The large majority of collisions are at very low  $Q^2$  values, where the photon is quasi-real, and are referred to as photoproduction reactions. The highest- $Q^2$  range is that of deep inelastic scattering (DIS). At intermediate  $Q^2$  values of the order of  $1 \text{ GeV}^2$ , there is a transition region.

While all interactions of the photon at HERA are assumed to be governed by QCD, the photoproduction and DIS regions exhibit different features.

The quasi-real photon may interact in two basic ways: it may couple immediately to a hard quark-antiquark pair, or it may interact by means of an intermediate partonic structure. The latter process, for quasi-real photons, is often modelled by means of the vector meson dominance hypothesis, in which the photon fluctuates into a mesonic state which then interacts with the proton. Hard scatters may then occur in which a parton originating from this state scatters off a parton from the proton. This scatter may be calculated in perturbative QCD, but the original fluctuation of the photon into a partonic state is not necessarily

calculable in this way. Hence the probability  $f_{a,\gamma}$  that a parton  $a$  is found with a fraction  $x_\gamma$  of the photon energy must often be obtained phenomenologically. Models based on a hadronic structure have been used, and also models based on fits to experimental data from photon-photon scattering.

In DIS, the partonic structure of the interacting photon is often taken to be entirely calculable in perturbative QCD. The non-perturbative component to the photon structure will then die away with  $Q^2$  through the transition region mentioned above. This region corresponds to the mass range of the vector mesons and the range below which perturbative methods in QCD may be expected to fail.

In this report, recent preliminary measurements by ZEUS of the resolved structure of the virtual photon are discussed. They are made over a wide  $Q^2$  range in an attempt to understand better the partonic behaviour of the photon.

## 2. TYPES OF PHOTON PROCESS

The basic types of hard photon process are illustrated in Fig. 1. In direct processes (a) the entire photon takes part in the hard interaction and there is no remnant in the photon direction. In resolved processes such as (b), the photon fluctuates into a state out of which a parton emerges to scatter off a parton from the proton. There is a photon remnant which takes the fraction of the photon energy which is not given to the hard scatter. This diagram indicates processes

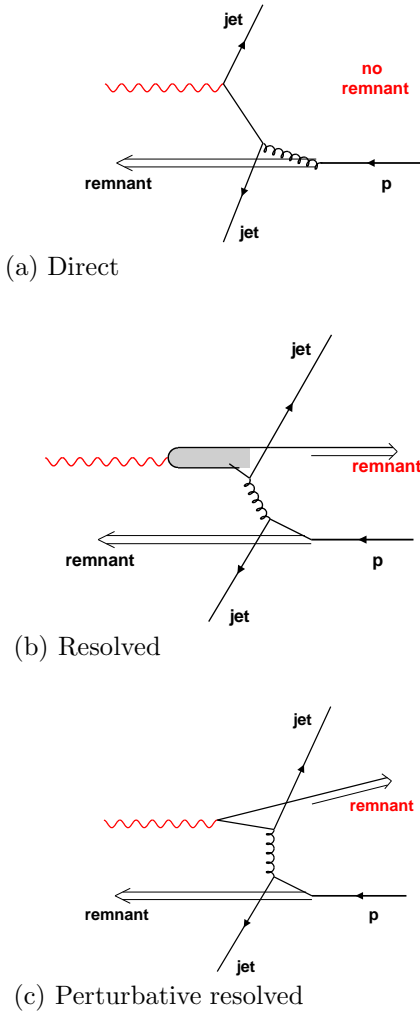


Figure 1. Examples of photon interactions.

in which the partonic state is non-perturbative in nature, and sometimes though controversially termed ‘hadronic’. The hard scatter itself, which produces the final-state jets, is of course calculable in perturbative QCD.

As depicted, (a) and (b) are lowest-order QCD diagrams with regard to the hard scatter, and the direct and resolved classes are separate. Corresponding diagrams at higher order can be drawn. While it is still often possible, for calculational purposes, to divide these into ‘direct’ and ‘re-

solved’ classes, more care is needed and the division between the two classes can become somewhat arbitrary.

Diagram (c) indicates a process in which the photon splits into a  $q\bar{q}$  pair, and which is NLO compared to (a). When this vertex involves a sufficiently high momentum transfer it is perturbatively calculable, as is the case if the  $q\bar{q}$  pair have a high  $p_T$  or if the incoming photon is highly virtual. A photon remnant is present, though not necessarily at low  $p_T$ , and only part of the photon energy is given to the final-state jets. This type of process may therefore be classed as resolved. In deciding whether to call the remaining photon system a remnant or a third jet, however, an arbitrary decision must be taken as to the  $p_T$  value that will constitute the boundary between the two cases.

The basic formula for calculating dijet cross sections in  $ep$  collisions can be written as

$$\begin{aligned}
 d\sigma_{ep \rightarrow e + \text{jets}} = & \\
 & \sum_{a,b} \int_0^1 dy f_{\gamma^*/e}(y, Q^2) \\
 & \times \int_0^1 dx_{\gamma^*} f_{a/\gamma^*}(x_{\gamma^*}, Q^2, \mu_{F\gamma^*}^2) \\
 & \times \int_0^1 dx_p f_{b/p}(x_p, \mu_{Fp}^2) d\sigma_{ab \rightarrow \text{jets}}(\mu_R).
 \end{aligned}$$

Here  $f_{\gamma^*/e}(y, Q^2)$  denotes the probability for the incoming  $e$  to radiate a given virtual photon, and  $f_{a/\gamma^*}$  and  $f_{b/p}$  denote the parton density functions (PDFs) of the photon and proton. The hypothesis of factorisation asserts that these are process-independent. For direct processes,  $f_{a/\gamma^*} = \delta(x_{\gamma^*} - 1)$ . In general there are two contributions to the resolved  $\gamma^*$  PDFs:

$$f_{a/\gamma^*} = f_{a/\gamma^*}^{\text{nonpert}} + f_{a/\gamma^*}^{\text{pert}}$$

The boundary between the non-perturbative and perturbative regions corresponds to the so-called ‘factorisation scale’  $\mu_F^2$ . The renormalisation scale  $\mu_R^2$  refers to the momentum transfer squared of the hard QCD scatter. In DIS,  $f_{a/\gamma^*}^{\text{nonpert}}$  is often assumed to be zero.

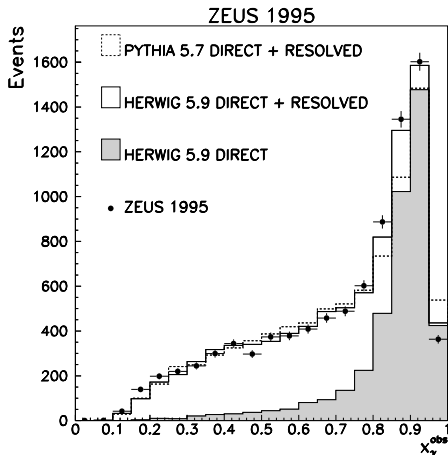


Figure 2. Typical distribution  $x_\gamma^{\text{obs}}$  observed in photoproduction at HERA. Calculated contributions are indicated from the resolved and direct processes at LO in the QCD scatter, with added initial and final state radiation.

### 3. DIJET EVENTS

In their recent analysis, ZEUS identify dijet events in the rear ( $\gamma^*$ ) hemisphere of the  $\gamma^*p$  centre-of-mass frame with  $E_T^{\text{jett}} > 7.5, 6.5$  GeV. A measure of  $x_\gamma$  is

$$x_\gamma^{\text{obs}} = (E_T^1 e^{-\eta_1} + E_T^2 e^{-\eta_2}) / 2E_{\gamma^*}$$

where the jets are labelled 1, 2 and  $\eta$  is pseudorapidity. Figure 2 shows a typical  $x_\gamma^{\text{obs}}$  distribution in photoproduction. The prominent peak is due largely to direct processes, while the tail is due largely to resolved processes; its precise shape depends on the cuts applied to the observed jets.

The incoming virtual photon energy  $E_{\gamma^*}$  is measured by tagging the scattered electron/positron in the ZEUS calorimeter system. A specially built calorimeter was inserted close to the beam line in order to enable  $Q^2$  values through the transition region to be studied.

A pure LO direct process has  $x_\gamma = 1$ , but the effects of initial and final state radiation and hadronisation reduce the value of the observed quantity. It is nevertheless useful to regard the regions  $x_\gamma^{\text{obs}} < 0.75$  and  $x_\gamma^{\text{obs}} > 0.75$  as

resolved-dominated and direct-dominated respectively. Provided the proton PDFs are known, the direct processes are reliably calculable in perturbative QCD, both in photoproduction and DIS. The present investigation is concerned primarily with the size of the resolved-dominated contribution as a function of  $Q^2$ . This can be studied by means of the ratio

$$R = \frac{d\sigma}{dQ^2}(x_\gamma^{\text{obs}} < 0.75) / \frac{d\sigma}{dQ^2}(x_\gamma^{\text{obs}} > 0.75)$$

A number of experimental and theoretical uncertainties tend to cancel in evaluating  $R$ , whose variation with the kinematics of the process may be used to study the behaviour of the effective partonic structure of the virtual photon.

The DISASTER++ Monte Carlo (D. Graudenz) was used to calculate parton cross sections at NLO. These were corrected to hadron level using the well-tried ARIADNE program. The data were corrected to hadron level using PYTHIA.

### 4. RESULTS

The measured cross section for the production of dijets, within the given kinematic acceptance, as a function of  $Q^2$ , is shown in Fig. 3. The data are compared to DISASTER calculations using a renormalisation scale  $\mu_R^2 = Q^2 + E_T^2$ , with  $\mu_{Fp}^2$  also set to this value. The dominant theoretical uncertainty was estimated by halving and doubling this value. DISASTER cannot be reliably used below a  $Q^2$  value of approximately 2 GeV<sup>2</sup>. It is of interest to see that DISASTER predicts the direct-dominated cross sections excellently, but underestimates the total cross section through a serious underprediction of the resolved-dominated component. A standard PDF is used for the proton, the results being insensitive to this choice. DISASTER evaluates only point-like photon processes, namely the direct and the perturbative resolved components. No non-perturbative photon PDF or photon factorisation scale therefore applies in this calculation.

A similar situation is observed when the cross sections are plotted as a function of the transverse jet energy  $E_T^{\text{jett}}$ . The underestimation of the cross sections is substantial and shows no strong  $E_T^{\text{jett}}$ -

dependence. As a further study, cross sections have been plotted as a function of the pseudo-rapidity of the more forward jet in the proton direction. DISASTER was also evaluated using  $\mu_R^2 = Q^2$ , although this is not a plausible choice for the present  $E_T^{\text{jet}}$  values unless  $Q^2 \gg (E_T^{\text{jet}})^2$ . It does, however, illustrate the sensitivity of the calculations to this scale.

Figure 4 shows the ratio  $R$ , plotted as a function of  $Q^2$  in three different  $(E_T^{\text{jet}})^2$  ranges (a-c). The value of  $R$  in photoproduction events ( $Q^2 \approx 0$ ), not plotted, is estimated to be similar, within errors, to the value for the lowest  $Q^2$  points shown.  $R$  is seen to fall sharply over the transition region for the lowest  $E_T^{\text{jet}}$  range, and more gently for the higher ranges. In (d),  $R$  is plotted in a different analysis in which dijet events containing a  $D^*$  meson were selected, and no fall in  $R$  is evident. The presence of either high  $E_T^{\text{jet}}$  or a heavy quark forces a high momentum scale on the QCD process. In such situations, the process is expected to be perturbatively calculable, with no prima facie reason for a strong  $Q^2$  dependence. The stronger fall-off at low  $E_T^{\text{jet}}$  values is consistent with the presence of strong non-perturbative photon structure effects in processes involving light quarks.

Nevertheless, even at high  $Q^2$ ,  $R$  does not fall to zero but seems to level off at a constant value that is not strongly dependent on  $E_T^{\text{jet}}$ . This may be interpreted in terms of an effective partonic structure to the photon, even at high virtualities. The DISASTER calculation, evaluated using  $\mu_R^2 = Q^2 + E_T^2$ , is unable to account for the data, and the discrepancy of the order of 50% does not vary strongly with the event kinematics. It is evident that the full cross section is not being correctly simulated by the perturbative model used. However the JETVIP model, although including a non-perturbative photon PDF, fares worse and cannot be considered competitive at present.

In an earlier study, H1 measured dijet events over a range of moderate  $Q^2$  values and interpreted the resolved cross sections in terms of an effective photon parton density (Fig. 5). This at first falls sharply from its value at  $Q^2 \approx 0$ ,

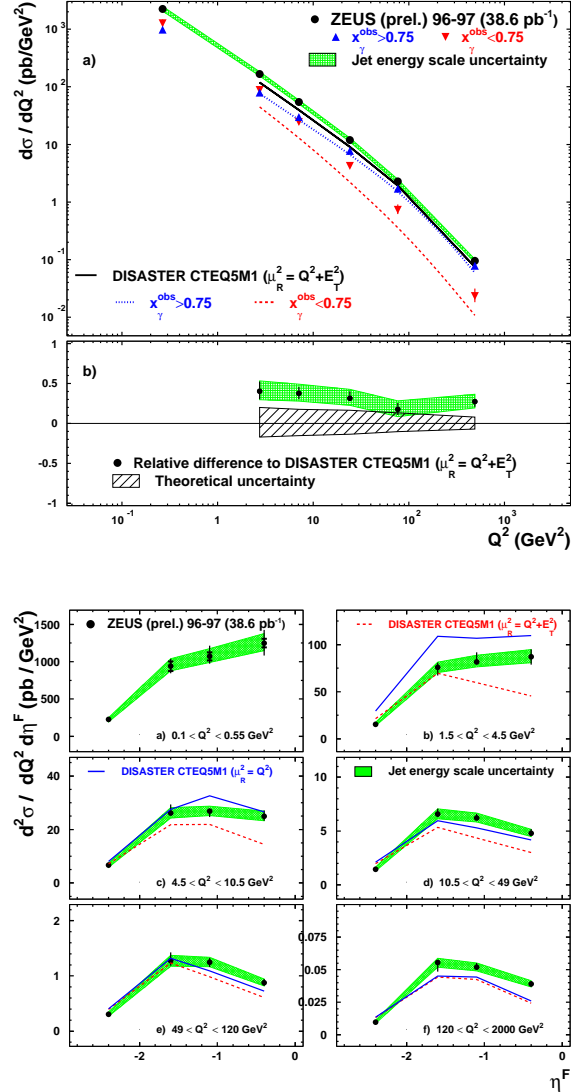


Figure 3. Upper plots: dijet cross sections as a function of  $Q^2$  of the virtual photon. Comparison is made with predictions from DISASTER for the direct and resolved dominated regions. Lower plots: cross sections as a function of pseudorapidity of the forward jet, for different  $Q^2$  regions. Comparison is made with predictions from DISASTER using two different renormalisation scales.

but afterwards remains constant within statistics. However, it was not possible to demonstrate a significant deviation from the falling NLO QCD calculation. The present ZEUS results appear to lend weight to the view that the effective parton structure of the photon remains approximately constant over this  $Q^2$  range.

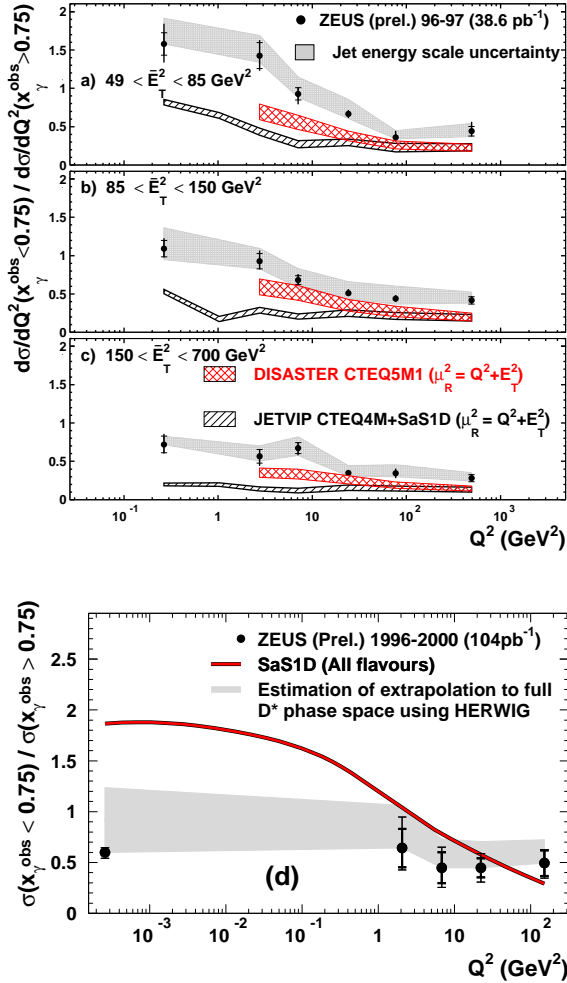


Figure 4. Cross section ratio  $R$  as a function of  $Q^2$  of the virtual photon, (a-c) in different ranges of  $(E_T^{\text{jet}})^2$ . Comparison is made with predictions from DISASTER and JETVIP. (d)  $R$  for events containing an identified  $D^2$  meson.

## 5. CONCLUSIONS

ZEUS has presented preliminary measurements of dijet cross sections over a range of  $Q^2$  values crossing the transition between photoproduction and DIS. A ratio of the resolved-dominated to direct-dominated cross sections is defined. It falls across this region, as the likely vector-meson dominated region of photon structure is left behind, but appears to attain a stable non-zero value. A component to the cross sections is indicated which is not modelled in the NLO QCD calculation DISASTER++. The shortfall is associated with resolved processes. Possible explanations might be a non-perturbative partonic structure in the photon even at high  $Q^2$ , or a surprisingly strong higher order perturbative contribution. The results are consistent with earlier H1 data. In events containing a charmed meson, the ratio does not fall with  $Q^2$ , but remains approximately flat over the entire range, at a similar value to the overall dijet sample at high  $Q^2$ .

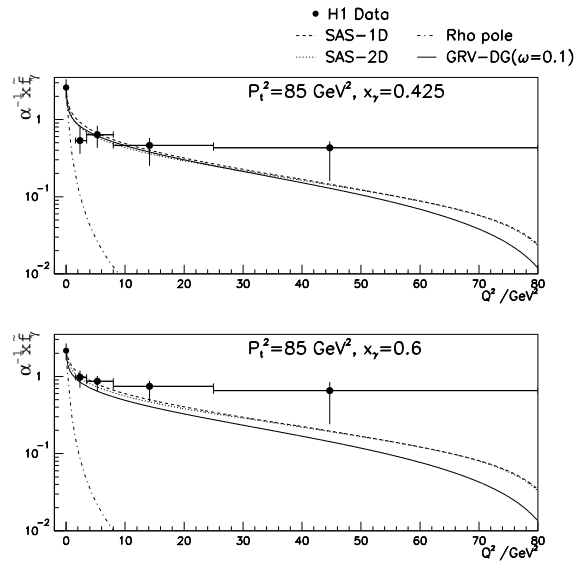


Figure 5. Effective parton density in the virtual photon, evaluated by H1, as a function of  $Q^2$ , compared with NLO predictions (Eur. Phys. J. C13 (2000) 397)